

CrystEngComm

Accepted Manuscript



This is an *Accepted Manuscript*, which has been through the Royal Society of Chemistry peer review process and has been accepted for publication.

Accepted Manuscripts are published online shortly after acceptance, before technical editing, formatting and proof reading. Using this free service, authors can make their results available to the community, in citable form, before we publish the edited article. We will replace this *Accepted Manuscript* with the edited and formatted *Advance Article* as soon as it is available.

You can find more information about *Accepted Manuscripts* in the [Information for Authors](#).

Please note that technical editing may introduce minor changes to the text and/or graphics, which may alter content. The journal's standard [Terms & Conditions](#) and the [Ethical guidelines](#) still apply. In no event shall the Royal Society of Chemistry be held responsible for any errors or omissions in this *Accepted Manuscript* or any consequences arising from the use of any information it contains.

ARTICLE

Reversible Recrystallization Process of Copper and Silver Thioacetamide-Halide Coordination Polymers and their Basic Building Blocks

Cite this: DOI: 10.1039/x0xx00000x

J. Troyano,^a J. Perles,^b P. Amo-Ochoa,^a J. I. Martínez,^c F. Zamora,^{a,*} and S. Delgado^{a,*}Received 00th January 2012,
Accepted 00th January 2012

DOI: 10.1039/x0xx00000x

www.rsc.org/

Three-dimensional [CuX(TAA)]_n (X=Br (1), I (2)) and bi-dimensional [AgX(TAA)]_n (X=Cl (3), Br (4)) coordination polymers have been isolated by direct synthesis between copper(I) and silver(I) halides and thioacetamide (TAA). These are multifunctional materials showing electrical conductivity (values at room temperature ranging from 7×10⁻⁶ to 2×10⁻⁹ S·cm⁻¹) and luminescent in the blue region. Unusual solubility of 1-4 in different solvents and recrystallization process observed for 1 and 2 in acetonitrile and for 3 and 4 in pyridine has been measured. We show preliminary results of the processability of 2 on glass for the production of organized thin films. These results are very attractive for the processability of coordination polymers in materials science and nanoscience.

Introduction

The study of coordination polymers (CPs) has gained major attention in recent years as an interface between synthetic chemistry and crystal engineering providing a solid foundation to help in the understanding of how molecules can be organized and how functions can be achieved.^{1-7,8} They give an intriguing way to assemble modular building units into designed networks whose structures and functions may be controlled by the geometry and functionality of the molecular components.^{9, 10} In addition, they show interesting properties including magnetism,¹¹ catalysis,^{10,12} non-linear optics,¹³ electrical conductivity¹⁴⁻¹⁷ and molecular sensing.^{18, 19} A wide range of one-, two- and three-dimensional architectures of CPs have been reported but the development of new structures is still of high interest due to the fact that they still can generate a variety of novel architectures with multifunctional properties. In terms of materials science the use of CPs is rather limited due to their processability.^{16, 20-22} Unlike molecular species, most CPs are insoluble once synthesised and so recrystallisation is not a choice. Typically, if the CPs can be dissolved, it is usually through the use of strongly coordinating solvents, which are then likely to become part of the recrystallized species, which therefore becomes a different material to the original one.²³

On the other hand, the use of organosulfur ligands in combination with metal ions is especially eye-catching for developing new metal-organosulfur networks showing electrical conductivity with potential applications in molecular electronics.^{24, 25} They have been explored as attractive building blocks for the design of multifunctional materials with

electronic properties including electrical, optical and magnetic.²⁶⁻³¹ In particular, the incorporation of thiolate-S as bridging ligands of transition metal sites in CPs seems to produce a synergic electronic effect since the orbital energies are better matched for S and there will be greater delocalization of spin density towards the bridging atom.³²

In this context, although heterocyclic thioamides constitute an important class of sulfur-containing organic compounds that have been largely studied for their interesting chemical, biochemical, structural and spectroscopic properties,³³ the aliphatic thioamides, such as the thioacetamide (TAA), have been scarcely developed. Thioamides are very versatile ligands in their coordination modes due to the presence of nitrogen and sulfur donor sites. They have the ability to behave as bidentate chelate or bridging ligands, or as monodentate “soft” ligands *via* S-coordination or “hard” ligands through N-site. Thus, in complexes of TAA with “soft” ions as copper(I) or silver(I) this ligand is competitive with “soft” anions such as the heavier halide ions. Additionally, the hydrogen bond interactions of amide groups play an essential role in proteins and polyamides,^{34, 35} however, they have received little attention in the field of supramolecular chemistry.³⁶ Surprisingly a recent revision in the CSD shows just three hits referred to CPs with aliphatic thioamides (Cd^{II},³⁷ Ni^{II},³⁸ and Cu^{I39}).

As we have previously established that CPs based on Cu(I) with organosulfur ligands are highly desirable to obtain materials with multifunctional properties,^{25, 40, 41} herein we focus in the potential of the TAA to produce new copper and silver CPs. Interestingly the four CPs characterized with Cu(I) and Ag(I)

show an unusual reversible recrystallization process. Their structural characterization and luminescent and electrical properties have been determined showing that these are multifunctional materials.

Results and discussion

Synthesis and Structure

The direct reactions between the corresponding metal halide salts of Cu(I) or Ag(I) and thioacetamide lead to crystalline materials of the corresponding CPs in high yield. Specifically the Cu(I) polymers, $[\text{CuX}(\text{TAA})]_n$ ($X = \text{Br}$ (**1**), I (**2**)), are isolated with bromine and iodine in acetonitrile, however, when the analogous reaction is carried out with CuCl the formation of a known molecular complex, $[\text{CuCl}(\text{TAA})]_3$, is observed.⁴² The structure of $[\text{CuCl}(\text{TAA})]_3$ had been previously reported (Fig. 1).⁴³ It consists of hexagonal Cu_3S_3 rings with Cl atoms acting as terminal ligands. These rings are located in layers parallel to the (110) plane and stacked along the [001] direction at a distance of 3.557 Å.

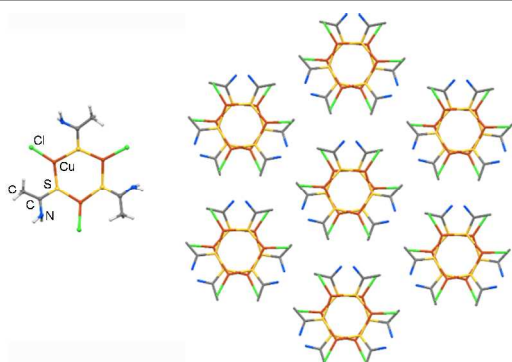


Figure 1. $\text{Cu}_3\text{S}_3\text{Cl}_3$ units present in the previously reported structure $[\text{CuCl}(\text{TAA})]_3$ (left); hexagonal packing of the columns of stacked rings along the (001) direction (right).

Compounds **1** and **2**, with formula $[\text{CuX}(\text{TAA})]_n$ ($X = \text{Br}$, I), display a 3D structure featuring with the same six-member cycles of alternating Cu and S atoms. However, the halogen ligands here act as bridges between these rings, giving rise to a polymeric structure. In this structural type, the copper atoms are coordinated in a tetrahedral environment surrounded by two sulfur atoms and two halogen atoms. The increase in coordination number, compared to the planar trigonal environment found in $[\text{CuCl}(\text{TAA})]_3$ allows the 3D connection of the rings. Like the situation found in the chlorine derivative, the organic ligands act as bridges between metal centres in such a disposition that they form hexagonal Cu_3S_3 rings parallel to the (110) plane, in which Cu and S atoms alternate. However, in **1** and **2**, these rings are joined along the [001] direction by Cu-X bonds in a non-planar honeycomb disposition, giving rise to the 3D structure. $\text{S}\cdots\text{S}$ interactions between sulfur atoms within the same ring are found in the structures of **1** and **2** ($\text{S}\cdots\text{S}$ distances around 3.65 Å). Considering the copper atoms and both types of ligands as nodes, the resulting 3-nodal 2,2,4-connected underlying net presents a new topology with point symbol $(12)(6.12^5)(6)$.

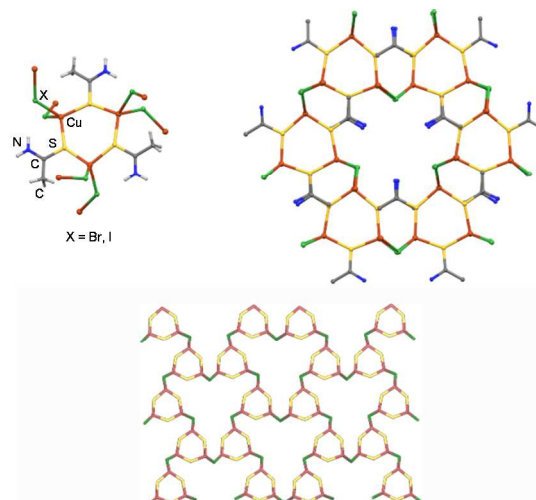


Figure 2. Ring found in the structures of **1** and **2** (top left), which is connected through bridging halogen ligands to six adjacent rings forming a non-planar honeycomb disposition (top right). Bottom: underlying net found in the structures of **1** and **2**; copper nodes are depicted in red, halogen nodes in green and thioacetamide nodes in yellow.

The analogous reactions carried out between TAA and AgX ($X = \text{Cl}$, Br) in a mixture of acetonitrile-water (4:1) allows to isolate the corresponding CPs $[\text{AgX}(\text{TAA})]_n$ ($X = \text{Cl}$ (**3**), Br (**4**)). Compounds **3** and **4** display a 2D polymeric structure with layers parallel to the (011) plane. They contain silver atoms coordinated in a tetrahedral environment to two sulfur atoms from the organic ligands, and two halogen atoms. As happened in the copper derivatives, both halogens and sulfur atoms act as bridges. Each type of bridging atoms join the metal atoms in perpendicular directions within the (011) plane: in these compounds the disposition of the sulfur and metal atoms does not allow the formation of rings, and as both bridging ligands join the metal centres in coplanar directions, the formation of a 3D structure is not possible. $[\text{AgX}(\text{TAA})]_n$ layers are joined by $\text{N-H}\cdots\text{Cl}$ interactions (distance $\text{N}\cdots\text{Cl} = 3.405$ Å).

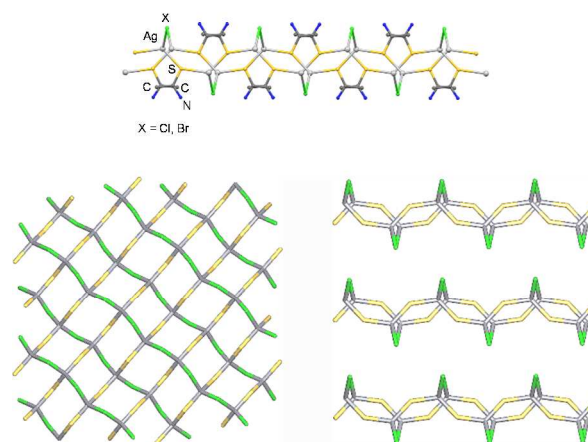


Figure 3. Side view of the double layer of compounds **3** and **4** (top). Bottom: underlying net in the structure of **3** and **4**, silver nodes are depicted in grey, halide nodes in green and thioacetamide nodes in yellow; left: view perpendicular to the layer and right: side view of the layer.

Table 1. Selected distances and angles for compounds 1-4.

	1	2	3	4
	Distances (Å)			
M-X	2.511(1) 2.514(1) 2.549(2) 2.549(2) 2.588(1) 2.591(1)	2.702(1) 2.702(1)	2.672(1) 2.672(1)	2.759(2) 2.770(2)
M-S	2.268(2) 2.273(2) 2.273(2) 2.274(2) 2.276(2) 2.277(2)	2.276(1) 2.292(1)	2.471(2) 2.536(2)	2.487(1) 2.547(1)
M-M	4.169(2) 4.175(2) 4.175(2) 4.658(2) 4.660(2) 4.660(2)	4.202(2) 4.937(2)	3.802(2) 4.720(2)	3.991(2) 4.752(2)
	Angles (°)			
S-M-S	106.67(7) 106.70(8) 106.72(7)	106.20(5)	125.38(3)	126.32(3)
X-M-X	97.63(3) 97.69(3) 97.63(3)	97.902(18)	88.14(5)	89.21(2)
S-M-X	113.09(7) 107.60(8) 117.65(7) 113.79(6) 110.03(1) 110.60(1) 114.69(8) 116.71(8) 106.72(7) 107.36(7) 114.52(7) 116.95(7)	110.86(5) 110.80(5) 115.55(5) 115.51(5)	104.10(3) 104.10(3) 4.21(3) 114.21(3)	104.5(2) 105.3(2) 112.0(2) 113.0(2)

The topological study performed upon this structure considering the metal atoms and the ligands as nodes gives rise to a 2,4-connected binodal net with point symbol $(8^4.12^2)(8)_2$, which also constitutes a new topology. A summary of selected bond distances and angles are collected in Table 1. Metal-metal distances are also shown in this table, although in all of the compounds they were found to be above the value required for M-M bonds. Metal centres joined by halogen atoms are closer to each other than centres joined by S atoms.

Physical Properties

ELECTRICAL CONDUCTIVITY

The structural features of CPs 1-4 showing Cu(I) or Ag(I) transition metal centres bridged by halides and sulphur atoms suggest that these materials may show electrical conductivity.²⁵ In particular three-dimensional CPs showing electrical conductivity are very limited.²⁵

Thus, two probe direct current (DC) electrical conductivity measurements at 300 K were performed in several single crystals of compounds 1-4. The conductivity values were obtained applying voltages from +10 V to -10 V. The average DC conductivity values for 1-4 at 300 K of 3×10^{-6} , 2×10^{-9} ,

7×10^{-6} and 2×10^{-7} S \cdot cm $^{-1}$, respectively, suggesting a semiconductor behaviour in all cases.

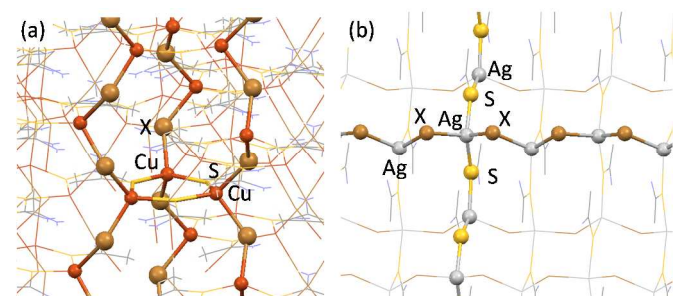


Figure 4. Representation of the different pathways connecting metal ions in compounds $[\text{CuX(TAA)}]_n$ (a) and $[\text{AgX(TAA)}]_n$ (b).

The 3D-CPs 1 and 2 show two different pathways connecting metal centres in their networks (Figure 4): i) Cu-X-Cu zig-zag chains along the *c* axis; and ii) Cu-X-Cu-S-Cu- pathway. The former are connecting the trinuclear $\text{Cu}_3(\text{TAA})_3$ entities. The shortest Cu-Cu distances through halide bridging ligands are *ca.* 4.17 and 4.20 Å (Table 1), for 1 and 2 respectively, while the shortest Cu-Cu distance bridged by S-atoms of the TAA, are *ca.* 4.66 and 4.94 Å for 1 and 2, respectively. The conductivity values of 1 and 2, of 3×10^{-6} and 2×10^{-9} , do not agree with the expected behavior based on the halide-metal orbitals coupling.²⁵ This fact suggests that the conductivity could probably be more favored by the Cu-X-Cu-S-Cu-pathway.

In compounds 3 and 4 the bidimensional structure is defined by two different zig-zag chains: i) Ag-X-Ag, and ii) Ag-S-Ag. The shortest Ag-Ag distances found for the halides bridging silver centres are *ca.* 3.80 and 4.00 Å, for 3 and 4 respectively, while in the chains mediated by TAA the shortest Ag-Ag distances are *ca.* 4.72 and 4.75 Å, respectively. In this case the better value of conductivity of 3 vs 4 can be easily explained since in both chains shorter metal-to-metal distances are found. Again the expected behavior based on the halide-metal orbitals coupling seems to be non-determinant in the electrical properties.

In order to rationalize these results, theoretical calculations have been carried out (further details in ESI). First, we have checked the transferability between the experimentally detected polymer geometries and the theoretical implementation. For that purpose we have performed, starting from the experimental configurations, full cell and structural DFT-based optimizations, where all the atoms were free to move and all the lattice parameters were free to relax. The results of the relaxation processes for all the polymer-bulks revealed no significant variations ($\sim 2\%$) with respect the starting geometries neither in the cell parameters (unit cell volume) nor in the structural arrangement, which enforces the accuracy of the theoretical framework used. The electronic structure calculations yield minimum values of the transport gaps at the Γ point of 0.57, 1.36, 2.15 and 2.07 eV for the $[\text{CuBr(TAA)}]_n$, $[\text{CuI(TAA)}]_n$, $[\text{AgCl(TAA)}]_n$ and $[\text{AgBr(TAA)}]_n$, respectively. Additionally, theory predicts (see density of electronic states in

Figure S19) the three-dimensional $[\text{CuBr(TAA)}]_n$ and $[\text{CuI(TAA)}]_n$ polymers as *p-type* semiconductors (with the Fermi level close to the valence band), and the bi-dimensional $[\text{AgCl(TAA)}]_n$ and $[\text{AgBr(TAA)}]_n$ polymers as *n-type* semiconductors (with the Fermi level close to the conduction band).

The theoretical results obtained for the transport gaps and semiconducting characters of the different coordination polymers can be rationalized in relation to the DC measured conductivities as follows: *i*) for the case of the $[\text{CuBr(TAA)}]_n$, the high value of its conductivity is directly related to its narrow transport gap (0.57 eV), independently of having a *p-type* semiconducting character, since the temperature and the applied voltage easily promote carriers towards the conduction band yielding a high conductivity of $3 \times 10^{-6} \text{ S cm}^{-1}$; *ii*) the case of the $[\text{CuI(TAA)}]_n$ is essentially different, since its *p-type* semiconducting character and wider value of the transport gap (1.36 eV) difficult the promotion of carriers towards the conduction band, yielding a low value of the conductance ($2 \times 10^{-9} \text{ S cm}^{-1}$); and, finally, *iii*) for the case of the 2D-CPs $[\text{AgCl(TAA)}]_n$ and $[\text{AgBr(TAA)}]_n$, in spite of showing the widest values of the transport gaps (2.15 and 2.07 eV, respectively), their *n-type* semiconducting character, with the Fermi level pinning up the conduction band, allows, by effect of the temperature and the moderately high value of the applied external voltage, to provide *available-for-the-conduction* carriers towards conduction band, yielding higher values of the conductivity with respect to the previous case (7×10^{-6} and $2 \times 10^{-7} \text{ S cm}^{-1}$, respectively).

LUMINESCENT PROPERTIES

Much research interest has recently focused on the luminescent properties of coordination polymers due to their potential applications as light emitting diodes.^{44,45,46} Particularly interesting among these are the derivatives of metal ions with d^{10} electronic configuration.^{47,48} Apart from metal-metal separations, the arrangement of the metal centres and the electronic structure of the molecule in the excited state are important to the photoluminescence behaviour of these polynuclear d^{10} metal complexes. In this context, Cu(I) complexes are particularly appropriate since they may show rich structural variety combined to brightly luminescent, even at room temperature, and emissive behaviour that can be modulated with structure and environment. On the contrary, the Ag(I) compounds are not usually emissive at room temperature or exhibit weak photoluminescence at around 480 nm.²³

The solid-state luminescent properties of molecular compound $[\text{CuCl(TAA)}]_3$ and $[\text{CuX(TAA)}]_n$ (X= Br (**1**), I (**2**)), $[\text{AgX(TAA)}]_n$ (X= Cl (**3**), Br (**4**)) were investigated in the solid state. Thus, at room temperature, excitation of solid samples at $\lambda = 359 \text{ nm}$ produces weak emission with two well defined peaks and maximum values centred at 416 and 469 nm that are assigned to the TAA ligand because they do not change from those observed for the free ligand (ESI, Figures S5 and S6). In general, possible assignments for the excited states that are responsible for emission phenomena of d^{10} complexes are

ligand-centred $\pi \rightarrow \pi^*$ transitions (LC), ligand-to-ligand (LLCT), ligand-to-metal (LMCT), or metal-to-ligand (MLCT) charge-transfer transitions or metal-centred $d^{10} \rightarrow d^9s^1$ (MCC) transitions.⁴⁹ The similar emission spectra observed between the thioacetamide ligand and all complexes suggests that these transitions could be assigned to ligand-centred $\pi \rightarrow \pi^*$ transitions and/or intraligands transitions since altering the metal did not affect the emission energy. In addition, weaker emission bands are observed for all complexes and may indicate the contribution of the halides in the emissive excited states, in the form of a MLCT or a halide to metal charge transfer (XMCT).⁵⁰ Contribution due to metal-centred $d^{10} \rightarrow d^9s^1$ (MCC) transitions are not possible because it is supported just by short metal-metal distances, and in compounds **1-4** these distances are longer than twice the van der Waals radius.⁵¹

Solution Studies and Processability

Coordination polymers have a high molecular weight based on the repetition of the basic sequence M-L, therefore they tend to have low or none solubility in most common solvents.²³ Certain cases of simple CPs have shown some solubility through breakup of the polymer and dissolution of their components.⁵² Additionally, we have recently found that some CPs based on MMX chains can show significant solubility. Thus platinum MMX chains are soluble in dichloromethane giving rise their two constituents building blocks MM and MMI_2 entities in a reversible way.^{20,53}

Based on these findings and in the structures found for **1-4**, in which M-X chains are present, we have studied their solubility in several solvents. The solubility of compounds **1-4** was calculated in several organic solvents by ^1H NMR spectroscopy (Experimental Section for details).⁵² We have observed that **1** and **2** are readily soluble in acetonitrile and methanol, while **3** and **4** are slightly soluble in both acetonitrile and methanol (Table 2).

The solubility has also been followed by UV-vis spectra. Thus, solutions of **1** and **2** in acetonitrile lead to a spectra in which an overlapping of the bands corresponding to the CuX and TAA species are clearly identified by comparison with the registered spectra of the free CuX and TAA under the same conditions (ESI, Figures S11-S13). Notice that the bands recorded in solid state for **1** and **2** at 230, 260, 271 and 286 nm are not observed in solution (ESI, Figure S10). Additional UV-vis studies carried out at variable temperature (20 °C to -40 °C) and concentration dependence (10^{-4} to 10^{-6} mol/L) do not allow to detect species of aggregation, oligomers. (ESI, Figures S16 and S17).

Table 2. Solubility of **1-4** in different solvents at 20°C (mmolL⁻¹ / gL⁻¹).

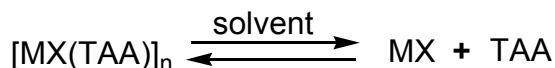
Solvents	1	2	3	4
acetonitrile	7.60/1.66	35.57/9.45	0.13/0.03	1.61/0.42
methanol	0.14/0.03	1.22/0.32	--	--

We have also studied the reversibility of the process trying to form the initial coordination polymers from these solutions (recrystallization of **1** and **2**). Thus, solubilisation of crystals of **1** and **2** leads to a solution containing the two constituent

building blocks of the CPs, namely CuX and TAA (Scheme 1). These solutions reverse to the starting materials, **1** and **2**, allowing their recrystallization (characterized by CNHS analysis, IR spectra and X-ray powder diffraction), upon concentration, by controlled solvent elimination, or cooling of the corresponding acetonitrile solutions.

Similar studies were carried out with **3** and **4**. In these cases the poor solubility of these materials in methanol and acetonitrile force us to use a more coordinate solvent (Table 2). Thus, pyridine solutions of **3** and **4** reverse to the initial crystalline CPs upon concentration or cooling (characterized by CNHS analysis, IR spectra and X-ray powder diffraction), confirming the reversibility of this process.

In principle, two key factors affecting the solubility of a CP are the bond strength of the coordinate bonds present in the CP structure, and the solubility of the building blocks, or subunits, generated in the solubilisation process or disassembles of the initial CP network. As shown in Table 2, the solubility values of **1-4** agree with both factors. Thus, **2** and **4** are more soluble than the corresponding analogues **1** and **3**, since the size of the halide favored both M-X bond strength and halide solvation. But even more important, the reversibility from the solution to the initial crystal formation is conditioned by the balance between the thermodynamic stability of the solvated building blocks and the formation of the CP in solid-state.



Scheme 1

Finally, in order to show the processability of these CPs we have selected the material with higher solubility. Thus, 100 μL of an acetonitrile solution of **2** (9 g/L) was drop-casted on a 1x1 cm^2 glass at 30 $^\circ\text{C}$ allowing solvent evaporation (*ca.* 4-5 min.). Optical inspection of the glass shows millimetric areas with apparent homogeneous covering.

The analysis of several area of this substrate by AFM analysis shows formation of over micron lengths thin film structures. Figure 5 shows a topographic AFM of a typical film displaying well-defined borders with heights *ca.* 1 μm and very smooth (roughness *ca.* 10-20 nm). X-ray powder diffraction of the film shows the peaks corresponding to those observed for **2** (Figure S18). This preliminary result show the potential to be organized using for instance soft-lithography.

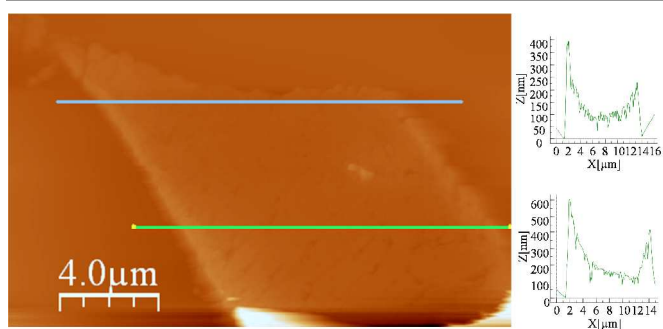


Figure 5. Topographic AFM image of the thin film formed by drop-casting in acetonitrile solution of compound **2** on a glass substrate. Height profiles along the blue and green lines (on the right).

Experimental

Materials and Methods. All the reagents were purchased from Sigma-Aldrich and used as received. The molecular compound $[\text{CuCl}(\text{TAA})]_3$ was prepared by a published method.⁴² FTIR spectra (KBr pellets) were recorded on a Perkin-Elmer 1650 spectrophotometer. C, H, N, S elemental analyses were performed by the Microanalysis Service of the Universidad Autónoma de Madrid on a Perkin-Elmer 240 B microanalyser. Electronic absorption spectra were recorded on an Agilent 8452 diode array spectrophotometer over a range of $\lambda=190\text{--}1100$ nm in 0.1, 0.2, and 1 cm quartz cuvettes thermostated by a Unisoku cryostat. Powder X-ray diffraction experiments were carried out on a Diffractometer PANalyticalX'Pert PRO theta/2theta primary monochromator and detector with fast X'Celerator. The samples have been analysed with scanning theta/2theta.

Direct current (DC) electrical conductivity measurements were performed on different single crystals of compounds **1-4**, with carbon paint at 300 K and two contacts. The contacts were made with wolframium wires (25 μm diameter). The samples were measured at 300 K applying an electrical current with voltages from +10 to -10 V.

Luminescence excitation and emission spectra of the solid compounds were performed at 25 $^\circ\text{C}$ on a 48000s (T-Optics) spectrofluorometer from SLM-Aminco. A front face sample holder was used for data collection and oriented at 60 $^\circ$ to minimize light scattering from the excitation beam on the cooled R-928 photomultiplier tube. Appropriate filters were used to eliminate Rayleigh and Raman scatters from the emission. Excitation and emission spectra were corrected for the wavelength dependence of the 450 W xenon arc excitation but not for the wavelength dependence of the detection system. Spectroscopic properties were measured by reflection (front face mode) on finely ground samples and placed in quartz cells of 1 mm path length. No attempt was made to remove adsorbed or dissolved molecular oxygen from the materials. Reference samples that do not contain any fluorescent dopant were used to check the background and optical properties of the samples.

Atomic Force Microscopy (AFM) images were acquired in dynamic mode using a Nanotec Electronica system operating at room temperature in ambient air conditions. For AFM measurements, Olympus cantilevers were used with a nominal

force constant of 0.75 N/m. The images were processed using WSxM.

X-ray Data Collection and Crystal Structure Determination. Data collection for compounds **1-4** was carried out on a Bruker Kappa Apex II diffractometer, using graphite-monochromated Mo-K α radiation ($\lambda=0.71073$ Å) and operating at 50 kV and 30 mA. The cell parameters were determined and refined by a least-squares fit of all reflections. A semi-empirical absorption correction (SADABS) was applied for all cases. The structures were solved by direct methods and refined by full-matrix least-square procedures on F² (SHELXL-97⁵⁴). All hydrogen atoms were included in their calculated positions and refined riding on the respective carbon atoms. Although in all of the structures the NH₂ group has a large degree of freedom, two alternative positions were found for N3 in the structure of compound **1** with a ratio of 61% and 39% occupancy. They were refined with a disorder model to a final good agreement. Further crystallographic details for the structures reported here may be obtained from the Cambridge Crystallographic Data Center, on quoting the depository numbers CCDC 990218-990221 (compounds **1-4**, respectively) Crystal and refinement data for **1-4** are collected in Table S1.

Measurements of the solubility of coordination polymers were based on the concentration of TAA in saturated solutions of the corresponding compounds as determined by ¹H NMR spectroscopy. To quantify the concentration of TAA in the saturated solution of coordination polymer, a known amount of 1,3,5-tribromobenzene was added to the saturated solutions as a standard. The concentration of TAA was then calculated by comparing the integral intensity of the corresponding NMR peaks of the methyl group of the TAA with the integral intensity of the peak of 1,3,5-tribromobenzene (in [D₄]methanol, 7.77 ppm, s, 3 H and [D₃]acetonitrile, 7.79 s, 3 H ppm).

Theoretical calculations have been carried out using Density Functional Theory (DFT)-based calculations (ESI for details).

Synthesis of [CuX(TAA)]_n [X= Br, (1), I (2)]. Thioacetamide (TAA) (0.120 g, 1.59 mmol) was added to a solution of CuX (X= Br, I) (1.49 mmol) in acetonitrile (10 mL) and the mixture was stirred at room temperature for 30 min. Then the solvent was removed under vacuum and the resulting pale yellow solid was washed with ethanol, acetonitrile and diethylether and dried under vacuum (0.256 g, 77 % yield for **1**, and 0.141 g, 36 % yield for **2** based on Cu). The purity of the samples was checked by X-ray powder diffraction. Single crystals of **1** and **2** suitable for X-ray diffraction studies were obtained after one day, by slow evaporation at room temperature of an acetonitrile solution of both polymers.

1: Anal. Calcd. (%) for C₂H₃BrCuNS: C, 10.99; H, 2.31; N, 6.41; S, 14.67. Found (%): C, 10.61; H, 2.39; N, 6.27; S, 14.59. IR selected data (KBr, cm⁻¹): 3477(s), 3286(s), 3139(s), 1636(s), 1478(m), 1408(m), 1367(m), 1297(s), 1028(w), 968(s), 697(s).

2: Anal. Calcd. (%) for C₂H₃ICuNS: C, 9.04; H, 1.90; N, 5.27; S, 12.07. Found (%): C, 8.78; H, 2.00; N, 5.27; S, 12.03. IR

selected data (KBr, cm⁻¹): 3333(s), 3273(s), 3169(s), 1627(s), 1475(m), 1403(m), 1370(m), 1303(m), 1025(w), 965(s), 696(s). **Synthesis of [AgX(TAA)]_n [X= Cl, (3), Br (4)].** A solution of AgNO₃ (0.162 g, 0.95 mmol) in acetonitrile (5 mL) was dropwise added, in darkness, to a mixture of KX (X= Cl, Br; 1.11 mmol) and TAA (0.089 g, 1.18 mmol) in 10 mL of acetonitrile:water (4:1). The suspension was stirred for 30 min at room temperature, and the grey solid was filtered, washed with water, acetonitrile and diethylether and dried under vacuum (0.120 g, 58 % yield for **3**, and 0.122 g, 49 % yield for **4**, based on Ag). The purity of the samples was checked by X-ray powder diffraction. Diffusion of diethylether into a pyridine solution of **3** and **4** compounds affords colourless crystals suitable for X-ray analysis.

3: Anal. Calcd. (%) for C₂H₃ClAgNS: C, 11.00; H, 2.31; N, 6.41; S, 14.68. Found (%): C, 10.45; H, 2.33; N, 6.39; S, 14.67. IR selected data (KBr, cm⁻¹): 3298(s), 3124(s), 1653(s), 1495(s), 1410(m), 1359(s), 1301(m), 1030(w), 970(s), 697(s).

4: Anal. Calcd. (%) for C₂H₃BrAgNS: C, 9.14; H, 1.92; N, 5.33; S, 12.20. Found (%): C, 8.73; H, 1.96; N, 5.32; S, 11.67. IR selected data (KBr, cm⁻¹): 3295(s), 3158(s), 1647(s), 1491(s), 1406(m), 1359(s), 1297(m), 1022(w), 968(s), 698(s).

Conclusions

In this work we have shown that the use of TAA as a bridging ligand can produce simple but interesting coordination polymers with multifunctional properties. The synthesized materials have increased the relative short list of 2D- and 3D-CPs showing electrical conductivity.

The use of coordination polymers in materials science is limited by their limited processability. Typically processability requires solubility of a polymer, and for CPs solubilisation lead to a decomposition of the initial material. There are a very limited number of samples of soluble CPs.²⁰ Very, recently we have demonstrated M-X bonds can help to the solubilisation process and in a reversibility way. This possibility has allowed the processability of these CPs for the production by wet-lithography of electrical conductive sub-micron structures and even an OFET device.^{20,53}

Interestingly, we have found that **1-4** show relatively high solubility in several low or no coordinating organic solvents and the ability to reverse from solution to the initial crystalline materials. These compounds represent the first samples of bi- and three-dimensional CPs showing a reversible recrystallization process. The processability showed by compound **2** strongly support the idea that these materials could be useful to produce new devices.

Acknowledgements

This work was supported by MICINN (MAT2010-20843-C02-01, CTQ2011-26507 and ACI2009-0969) and Comunidad de Madrid (CAM2009-S2009-MAT-1467). Authors are indebted with Dr. M. Zayat (ICCM-CSIC, Spain) for their assistance in luminescence measurements. JIM acknowledges funding from the CSIC-JaeDoc Fellowship Program.

Notes and references

^a Departamento de Química Inorgánica, Universidad Autónoma de Madrid, E-28049 Madrid, Spain. E-mail: felix.zamora@uam.es, salome.delgado@uam.es. Homepage: www.nanomater.es.

^b Servicio Interdepartamental de Ayuda a la Investigación. Unidad de rayos-X. Universidad Autónoma de Madrid, E-28049 Madrid, Spain.

^c Departamento Superficies y Recubrimientos, Instituto de Ciencia de Materiales de Madrid (ICMM-CSIC), E-28049 Madrid, Spain.

Electronic Supplementary Information (ESI) available: Crystallographic Table of Crystal data and structure refinement and additional UV-vis, emission spectra, X-ray powder diffractograms, electrical measurements I/V graphics and details of theoretical calculations. See DOI:10.1039/b000000x/

- S. Kitagawa and S. Noro, *In Comprehensive Coordination Chemistry II*, Elsevier, Amsterdam, 2004.
- B. Moulton and M. J. Zaworotko, *Chem. Rev.*, 2001, **101**, 1629-1658.
- N. Stock and S. Biswas, *Chem. Rev.*, 2012, **112**, 933-969.
- S. T. Meek, J. A. Greathouse and M. D. Allendorf, *Adv. Mater.*, 2011, **23**, 249-267.
- W. L. Leong and J. J. Vittal, *Chem. Rev.*, 2011, **111**, 688-764.
- C. Janiak and J. K. Vieth, *New J. Chem.*, 2010, **34**, 2366-2388.
- D. J. Tranchemontagne, J. L. Mendoza-Cortes, M. O'Keefe and O. M. Yaghi, *Chem. Soc. Rev.*, 2009, **38**, 1257-1283.
- M. Hong, *Cryst. Growth Des.*, 2007, **7**, 10-14.
- Y. Liu, W. M. Xuan and Y. Cui, *Adv. Mater.*, 2010, **22**, 4112-4135.
- S. Kitagawa, R. Kitaura and S. Noro, *Angew. Chem. Int. Ed.*, 2004, **43**, 2334-2375.
- L. Brammer, *Chem. Soc. Rev.*, 2004, **33**, 476-489.
- A. Corma, H. Garcia and F. X. L. I. Llabres i Xamena, *Chem. Rev.*, **110**, 4606-4655.
- H. W. Hou, X. R. Meng, Y. L. Song, Y. T. Fan, Y. Zhu, H. J. Lu, C. X. Du and W. H. Shao, *Inorg. Chem.*, 2002, **41**, 4068-4075.
- R. Mas-Balleste, J. Gomez-Herrero and F. Zamora, *Chem. Soc. Rev.*, 2010, **39**, 4220-4233.
- E. Mateo-Marti, L. Welte, P. Amo-Ochoa, P. J. S. Miguel, J. Gomez-Herrero, J. A. Martin-Gago and F. Zamora, *Chem. Commun.*, 2008, 945-947.
- D. Olea, S. S. Alexandre, P. Amo-Ochoa, A. Guijarro, F. de Jesus, J. M. Soler, P. J. de Pablo, F. Zamora and J. Gomez-Herrero, *Adv. Mater.*, 2005, **17**, 1761-1765.
- L. Welte, U. Garcia-Couceiro, O. Castillo, D. Olea, C. Polop, A. Guijarro, A. Luque, J. M. Gómez-Rodríguez, J. Gómez-Herrero and F. Zamora, *Adv. Mater.*, 2009, **21**, 2025-2028.
- J. R. Long, L. G. Beauvais and M. P. Shores, *J. Am. Chem. Soc.*, 2000, **122**, 2763-2772.
- R. Mas-Balleste, G. Gomez-Navarro, J. Gomez-Herrero and F. Zamora, *Nanoscale*, 2011, **3** 20-30.
- D. Gentili, G. Givaja, R. Mas-Balleste, M. R. Azani, A. Shehu, F. Leonardi, E. Mateo-Marti, P. Greco, F. Zamora and M. Cavallini, *Chem. Sci.*, 2012, **3**, 2047-2051.
- D. Olea, R. Gonzalez-Prieto, J. L. Priego, M. C. Barral, P. J. de Pablo, M. R. Torres, J. Gomez-Herrero, R. Jimenez-Aparicio and F. Zamora, *Chem. Commun.*, 2007, 1591-1593.
- U. Garcia-Couceiro, D. Olea, O. Castillo, A. Luque, P. Roman, P. J. de Pablo, J. Gomez-Herrero and F. Zamora, *Inorg. Chem.*, 2005, **44**, 8343-8348.
- C. Janiak, *Dalton Trans.*, 2003, 2781-2804.
- H.-B. Zhu and S.-H. Gou, *Coord. Chem. Rev.*, 2011, **255**, 318-338.
- G. Givaja, P. Amo-Ochoa, C. J. Gomez-Garcia and F. Zamora, *Chem. Soc. Rev.*, 2012, **41**, 115-147.
- J. A. Garcia-Vazquez, J. Romero and A. Sousa, *Coord. Chem. Rev.*, 1999, **193-5**, 691-745.
- P. C. Ford and A. Vogler, *Acc. Chem. Res.*, 1993, **26**, 220-226.
- E. S. Raper, *Coord. Chem. Rev.*, 1996, **153**, 199-255.
- E. S. Raper, *Coord. Chem. Rev.*, 1997, **165**, 475-567.
- P. D. Akrivos, *Coord. Chem. Rev.*, 2001, **213**, 181-210.
- T. S. Lobana, R. Sharma, E. Bermejo and A. Castineiras, *Inorg. Chem.*, 2003, **42**, 7728-7730.
- S. S. Alexandre, J. M. Soler, P. J. Sanz Miguel, R. W. Nunes, F. Yndurain, J. Gomez-Herrero and F. Zamora, *Appl. Phys. Lett.*, 2007, **90**.
- T. S. Lobana, R. Sharma, G. Bawa and S. Khanna, *Coord. Chem. Rev.*, 2009, **253**, 977-1055.
- E. N. Baker and R. E. Hubbard, *Prog. Biophys. Mol. Bio.*, 1984, **44**, 97-179.
- N. S. Murthy, *J. Polym. Sci. Pol. Phys.*, 2006, **44**, 1763-1782.
- T. Mes, S. Cantekin, D. W. R. Balkenende, M. M. M. Frissen, M. A. J. Gillissen, B. F. M. De Waal, I. K. Voets, E. W. Meijer and A. R. A. Palmans, *Chem. Eur. J.*, 2013, **19**, 8642-8649.
- M. M. Rolies and C. J. Deranter, *Acta Crystall. B*, 1978, **34**, 3216-3218.
- L. Capacchi, G. F. Gasparri, M. Nardelli and G. Pelizzi, *Acta Cryst.*, 1968, **B24**, 1199-1204.
- F. B. Stocker and M. A. Troester, *Inorg. Chem.*, 1996, **35**, 3154-3158.
- S. Delgado, P. J. S. Miguel, J. L. Priego, R. Jimenez-Aparicio, C. J. Gomez-Garcia and F. Zamora, *Inorg. Chem.*, 2008, **47**, 9128-9130.
- A. Gallego, O. Castillo, C. J. Gomez-Garcia, F. Zamora and S. Delgado, *Inorg. Chem.*, 2012, **51**, 718-727.
- R. R. Iyengar, D. N. Sathyanarayana and C. C. Patel, *J. Inorg. Nucl. Chem.*, 1972, **34**, 1088-1091.
- C. J. De Ranter and M. Rolies, *Cryst. Struct. Comm.*, 1977, **6**.
- E. Cariati, X. H. Bu and P. C. Ford, *Chem. Mater.*, 2000, **12**, 3385-3391.
- D. M. Ciurtin, N. G. Pschirer, M. D. Smith, U. H. F. Bunz and H. C. zur Loye, *Chem. Mater.*, 2001, **13**, 2743-2747.
- F. Wurthner and A. Sautter, *Chem. Commun.*, 2000, 445-446.
- H. A. Habib, A. Hoffmann, H. A. Hoeppe, G. Steinfeld and C. Janiak, *Inorg. Chem.*, 2009, **48**, 2166-2180.
- V. W.-W. Yam and K. M.-C. Wong, *Chem. Commun.*, 2011, **47**, 11579-11592.
- V. W. W. Yam and K. K. W. Lo, *Chem. Soc. Rev.*, 1999, **28**, 323-334.
- P. C. Ford, E. Cariati and J. Bourassa, *Chem. Rev.*, 1999, **99**, 3625-3647.
- A. Bondi, *J. Phys. Chem.*, 1964, **68**, 441-&.
- X. J. Cui, A. N. Khlobystov, X. Y. Chen, D. H. Marsh, A. J. Blake, W. Lewis, N. R. Champness, C. J. Roberts and M. Schroder, *Chem. Eur. J.*, 2009, **15**, 8861-8873.

53. A. P. Paz, L. A. Espinosa Leal, M. R. Azani, A. Guijarro, P. J. S. Miguel, G. Givaja, O. Castillo, R. Mas-Balleste, F. Zamora and A. Rubio, *Chem. Eur. J.*, 2012, **18**, 13787-13799.
54. G. M. Sheldrick, *SHELXL-97, Program for Crystal Structure Refinement*; Universität Göttingen., 1997.